AGU PUBLICATIONS

Geophysical Research Letters

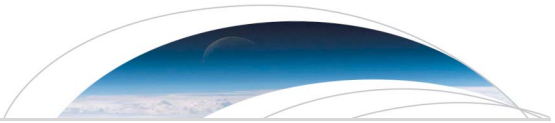

RESEARCH LETTER

10.1002/2015GL064795

Key Points:
- The temperature dependence of the zeta potential is explained by the temperature dependence of pH
- At low salinity, pH decreases with increasing temperature but is independent of T at high salinity
- We present a model that explains the hitherto contradictory results reported in previous studies

Supporting Information:
- Supporting Information S1
- Data Set S1
- Data Set S2
- Data Set S3
- Table S1
- Table S2

Correspondence to:
J. Vinogradov,
j.vinogradov@imperial.ac.uk

Citation:
Vinogradov, J., and M. D. Jackson (2015), Zeta potential in intact natural sandstones at elevated temperatures, *Geophys. Res. Lett.*, *42*, 6287–6294, doi:10.1002/2015GL064795.

Received 15 JUN 2015
Accepted 8 JUL 2015
Accepted article online 14 JUL 2015
Published online 13 AUG 2015

Zeta potential in intact natural sandstones at elevated temperatures

Jan Vinogradov[1] and Matthew D. Jackson[1]

[1]Department of Earth Science and Engineering, Imperial College London, London, UK

Abstract We report measurements of the zeta potential of natural sandstones saturated with NaCl electrolytes of varying ionic strengths at temperatures up to 150°C. The zeta potential is always negative but decreases in magnitude with increasing temperature at low ionic strength (0.01 M) and is independent of temperature at high ionic strength (0.5 M). The pH also decreases with increasing temperature at low ionic strength but remains constant at high ionic strength. The temperature dependence of the zeta potential can be explained by the temperature dependence of the pH. Our findings are consistent with published models of the zeta potential, so long as the temperature dependence of the pH at low ionic strength is accounted for and can explain the hitherto contradictory results reported in previous studies.

1. Introduction

The zeta potential is a measure of the electrical potential of the mineral surfaces in water-saturated rocks. Its magnitude and polarity control the electrostatic interactions between mineral surfaces and polar species in aqueous solution, and also the magnitude and polarity of the self-potential resulting from electrokinetic processes. In many subsurface settings, including geothermal fields [*Corwin and Hoover*, 1979; *Fitterman and Corwin*, 1982; *Ishido et al*., 1989; *Revil and Pezard*, 1998; *Darnet et al*., 2004; *Jardani et al*., 2008], deep saline aquifers [*Moore et al*., 2004; *Ishido et al*., 2013], hydrocarbon reservoirs [*Gulamali et al*., 2011; *Saunders et al*., 2012], volcanoes [*Aubert and Atangana*, 1996; *Michel and Zlotnicki*, 1998; *Revil et al*., 2011], and during seismoelectric exploration [*Revil and Mahardika*, 2013], the rocks are at elevated temperature; yet the temperature dependence of the zeta potential remains poorly understood [*Glover*, 2015]. There are very few previous experimental studies, and these report inconsistent and contradictory behavior; some studies have found that the zeta potential increases in magnitude with increasing temperature, while others have found that it decreases in magnitude (e.g., Figure 1). Moreover, few studies have investigated salt concentrations relevant to natural systems; most used deionized water or NaCl/KCl electrolytes at low ionic strength (10^{-3} M; 1 M = 1 mol dm^{-3}; see Figure 1 and Table S1 in the supporting information). Natural groundwater is typically more saline than this. The aim of this study is to determine the temperature dependence of the zeta potential in natural sandstones over the range 23–150°C, saturated with NaCl electrolytes of 0.01 M (comparable to potable water) and 0.5 M (comparable to seawater) ionic strength.

2. Materials and Methods

We use the streaming potential method described by *Vinogradov et al*. [2010] to determine the zeta potential of intact natural sandstone samples. The experimental setup is modified from that described by *Jaafar et al*. [2009] and *Vinogradov et al*. [2010] to allow measurements at elevated temperature (see Figure S1 in the supporting information). The core holders containing the sample, the reservoirs (columns) that supply the electrolyte to the sample, and the electrodes used to measure the electrical potential across the sample, were placed in an oven with temperature controlled to ±0.5°C. The pump used to flow the electrolyte through the sample remained outside of the oven, and the electrolyte was forced from one reservoir, through the sample, and into the other reservoir, by using Multipar oil as a hydraulic fluid and flow lines that pass through the wall of the oven from the reservoirs to the pump. For temperatures in the range 18–80°C, the pH and electrical conductivity of the NaCl electrolyte were measured inside the oven using a Mettler Toledo pH meter and a Metrohm 712 conductometer, respectively. The electrical conductivity of the saturated rock specimen was measured over the entire temperature range investigated using the approach of *Vinogradov and Jackson* [2011].

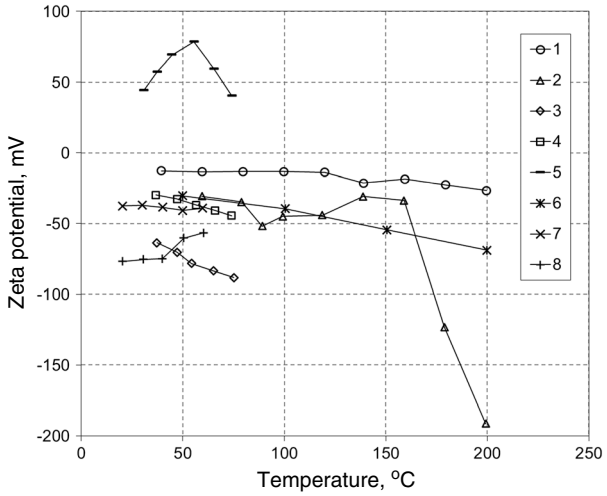

Figure 1. Summary of all published experimental data for the temperature dependence of zeta potential. Data sets: 1 and 2—*Reppert and Morgan* [2003]; 3, 4, and 5—*Ishido and Mizutani* [1981]; 6—*Alekhin et al.* [1984]; 7 and 8—*Dunstan* [1994]. More detailed information can be found in Table S1 in the supporting information.

The saturated samples were placed in the sample holder inside a Viton sleeve of 2 mm wall thickness and a confining pressure of about 1.4 MPa above atmospheric was applied. The sleeve is capable of withstanding temperatures up to 150°C. A backpressure was applied to the fluids in the reservoirs of about 50 kPa above the temperature-dependent water boiling pressure. The samples were cleaned using the Soxhlet extraction procedure described by *Jackson and Vinogradov* [2012], saturated under vacuum with the electrolyte of interest and loaded into the sample holder. The electrolyte was flowed repeatedly through the sample from one reservoir to the other and back again while periodically measuring the pH and conductivity of the electrolyte, until the pH and conductivity remained constant within a 5% tolerance (typically over 24–48 h). The final measured values represent the equilibrium pH and electrolyte conductivity at laboratory temperature. The sample was then brought to the temperature of interest and left to equilibrate for a further 24–48 h, after which the electrolyte was again flowed repeatedly through the sample from one reservoir to the other and back again for 4–5 h, to confirm that the pH and conductivity at the temperature of interest remained constant within a 5% tolerance. The final measured values represent the equilibrium pH and electrolyte conductivity at the temperature of interest. Streaming potential measurements then commenced.

The streaming potential was measured using the "paired-stabilization" (PS) method of *Vinogradov and Jackson* [2011]. In this method, the pump is used to flow the electrolyte through the sample at constant rate until stable pressure and voltage (varying by less $<3\%$ of the measured value over a period varying from 30 s to 20 min depending on sample permeability) are recorded across the sample (e.g., Figure S2a in the supporting information). The flow direction is then reversed at the same rate. A symmetric response confirms that electrode polarization effects are small and that the measured electrical potential corresponds to the streaming potential. These PS experiments are repeated at three or four different flow rates and the stabilized voltage for each experiment plotted as a function of the stabilized pressure difference (e.g., Figure S2b in the supporting information). The gradient of a linear regression through these data yields the streaming potential coupling coefficient (C_{sp}), which is related to the zeta potential (ζ) via a modified version of the Helmholtz-Smoluchowski equation that accounts for surface electrical conductivity. This modification was first proposed by *Fairbrother and Mastin* [1924] and later used by many authors [see, for example, *Jouniaux and Pozzi*, 1995; *Glover*, 2015]

$$C_{sp} = \frac{\Delta V}{\Delta P} = \frac{\varepsilon \zeta}{\mu \sigma_r F} \tag{1}$$

Here μ is the dynamic viscosity of the electrolyte, ε is the permittivity of the electrolyte, σ_r is the conductivity of the sample saturated with the electrolyte at experimental conditions, and F is the intrinsic formation factor of the sample. We obtained μ and ε as a function of temperature and ionic strength using the approach of *Saunders et al.* [2012] (see his Appendix A). The sample conductivity σ_r was measured before and after each streaming potential measurement using the approach reported in *Vinogradov et al.* [2010] (Figure 2a). The intrinsic formation factor F along with other key sample data was available from previous studies, including measurements of streaming potential for single and multiphase flow at laboratory temperature [*Jaafar et al.*, 2009; *Vinogradov et al.*, 2010; *Leinov and Jackson*, 2014] (see Table S2 in the supporting information). The electrolytes were prepared by dissolving NaCl salt in deionized water obtained from a Barnstead TII (Thermo Scientific) water system with an electrical resistivity >15 MΩ cm.

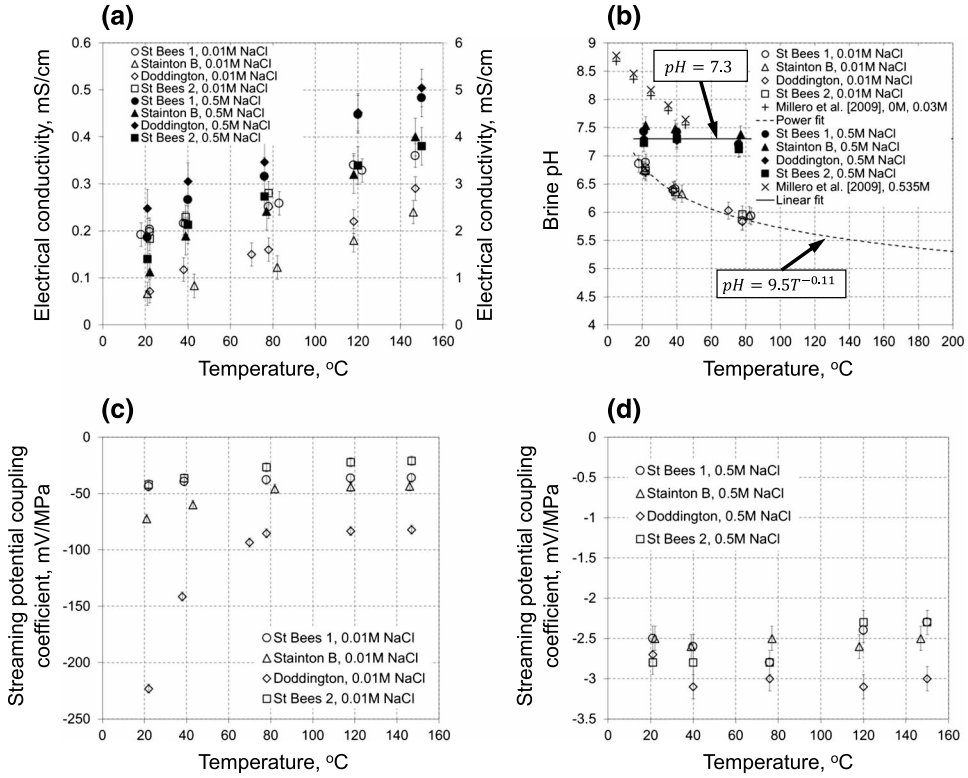

Figure 2. Experimental results. (a) Electrical conductivity of the saturated samples as a function of temperature: solid symbols denote 0.5 M NaCl electrolyte and are plotted against the right-hand axis; open symbols denote 0.01 M NaCl electrolyte and are plotted against the left-hand axis. (b) Brine pH as a function of temperature: solid symbols and the solid line denote 0.5 M NaCl electrolyte; open symbols and the dashed line denote 0.01 M NaCl electrolyte. Also shown are the results from *Millero et al*. [2009] for two NaCl electrolytes. (c) Streaming potential coupling coefficient as a function of temperature for 0.01 M NaCl electrolyte. (d) Streaming potential coupling coefficient as a function of temperature for 0.5 M NaCl electrolyte.

3. Results

Typical results of the PS experiments are shown in Figure S2 in the supporting information. Figure 2a shows the measured electrical conductivities of all samples saturated with 0.01 M (hollow symbols) and 0.5 M NaCl (filled symbols). These data show increasing conductivity with temperature, higher conductivity for the more concentrated 0.5 M electrolyte, and higher conductivity for the higher-porosity samples, consistent with previous studies [e.g., *Glover and Déry*, 2010; *Vinogradov et al*., 2010]. Figure 2b shows measurements of the electrolyte pH at temperatures up to 80°C. For the 0.01 M electrolyte, we observe a decrease in pH with increasing temperature; a similar relationship between pH and temperature for NaCl electrolyte has been observed previously [*Millero et al*., 2009]. However, the pH of the 0.5 M electrolyte is constant within experimental error. We model the temperature dependence of the pH for the 0.01 M electrolyte using a power law fitted to the data given by

$$\mathrm{pH} = 9.5T^{-0.11} \tag{2}$$

with a quality of fit of $R^2 = 0.98$. We have assumed the pH of the 0.5 M electrolyte is constant at 7.3 which fits all of the measured data within experimental error.

Figures 2c and 2d show the temperature dependence of the coupling coefficient at NaCl ionic strength of 0.01 M and 0.5 M, respectively. We find that the coupling coefficient is negative regardless of temperature, rock sample, or ionic strength. However, at the lower ionic strength (0.01 M), the coupling coefficient decreases in magnitude with increasing temperature and there is considerable spread between samples, with the Doddington sample showing the largest magnitude and greatest temperature dependence, and the St. Bees samples showing the smallest magnitude and least temperature dependence (Figure 2c). At the higher ionic strength (0.5 M), the magnitude of the coupling coefficient is much smaller (compare vertical axis scales on Figures 2c and 2d) and there is little or no temperature dependence within experimental error,

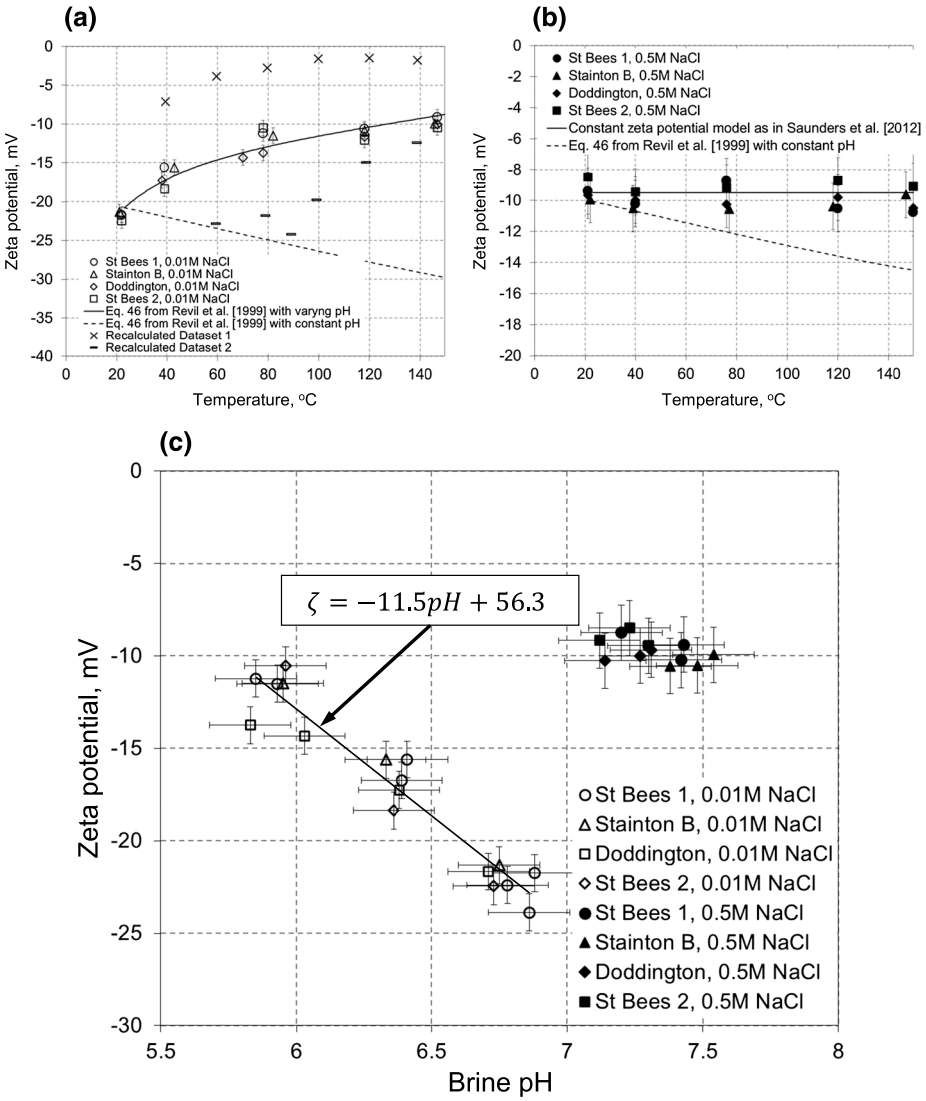

Figure 3. Zeta potential as a function of (a) temperature for 0.01 M NaCl electrolyte, (b) temperature for 0.5 M electrolyte, and (c) pH for both electrolytes.

although the different samples record different magnitudes (Figure 2d). For all samples, and irrespective of ionic strength, the measured values of the coupling coefficient at laboratory temperature (23°C) are consistent with those obtained previously using the same samples [*Jaafar et al.*, 2009; *Vinogradov et al.*, 2010].

We finish by reporting the values of zeta potential obtained using the data recorded in Figures 2a, 2c, 2d, and equation (1). Despite the spread in values of the coupling coefficient obtained for the different samples, we find the zeta potential collapses onto a common trend for each of the two ionic strengths investigated (Figures 3a and 3b). At the lower ionic strength (0.01 M; Figure 3a), the zeta potential consistently decreases in magnitude with increasing temperature, while at the higher ionic strength (0.5 M; Figure 3b), the zeta potential shows no temperature dependence outside experimental error. In all cases, the zeta potential is negative, consistent with negatively charged mineral surfaces as observed in numerous previous studies of natural sandstones saturated with NaCl electrolyte at laboratory temperature [see *Walker et al.*, 2014, and references therein] and in the few studies that investigated elevated temperature (Figure 1).

4. Discussion

We find a clear and consistent temperature dependence of the zeta potential in natural sandstones saturated with NaCl electrolyte which is the same across the three different sandstones investigated here but depends

on the ionic strength of the electrolyte. At the lower ionic strength tested (0.01 M), we find that the zeta potential decreases in magnitude with increasing temperature, while at the higher ionic strength tested (0.5 M), we find that the zeta potential remains constant within experimental error.

Previous studies have tested natural sandstones or silica particles saturated with distilled water, or NaCl/KCl/KNO_3 electrolytes at low ionic strength (10^{-3} M; see Figure 1 and Table S1 in the supporting information). We compare these studies against the data obtained here at 0.01 M ionic strength. *Dunstan* [1994] obtained a similar trend of zeta potential decreasing in magnitude with increasing temperature in colloidal silica particles saturated with ultrapure water (data set 8 in Figure 1 and Table S1); they also recorded a decrease in pH from 6 to 5.1, consistent with our observation. However, they observed no trend in the same material saturated with 10^{-3} M KCl (data set 7 in Figure 1 and Table S1). By contrast, *Reppert and Morgan* [2003] found the opposite trend in Fontainebleau sandstone saturated with deionized water, and Berea sandstone saturated with 10^{-3} M NaCl electrolyte (data sets 1 and 2, respectively, in Figure 1 and Table S1). In these experiments, the pH was unbuffered and showed a decrease from 8.1 to 5.5 for the Fontainebleau sample, and from 8.3 to 6 for the Berea sample; note that the pH was always measured at laboratory conditions, before and after the elevated temperature measurement. *Ishido and Mizutani* [1981] similarly found that the zeta potential increased in magnitude with increasing temperature in crushed quartz saturated with 10^{-3} M KNO_3 electrolyte, but they kept the pH fixed and investigated two different values of pH = 4.2 and 6.1 (data sets 3–5 in Figure 1 and Table S1), while *Alekhin et al*. [1984] observed the same trend of increasing zeta potential in powered silica samples saturated with 10^{-3} M NaCl electrolyte with a fixed pH = 4 (data set 6 in Figure 1 and Table S1).

We compare our zeta potential measurements obtained at 0.01 M ionic strength with the model of *Revil et al*. [1999] (specifically, their equations 34 and 46). We use the temperature dependence of pH given in equation (2), and values of $K_{Me} = 10^{-7.5}$, $K_{(-)} = 10^{-7}$, and $\Gamma^0_S = 4\,\mathrm{nm}^{-2}$ which are typical for silica in contact with NaCl electrolyte and similar to those used by *Revil et al*. [1999] and *Saunders et al*. [2012]. We assume that concentration and ionic strength are identical (i.e., the NaCl electrolyte behaves as an ideal electrolyte) and that concentration of acids is negligible. We also assume that the shear plane is located at $\chi_\zeta = 3.64$ nm, which can be compared to the Debye length of $\chi_d = 3.03$ nm calculated for this ionic strength [see *Jackson*, 2015]. Also shown for comparison is the model prediction assuming constant pH = 6.73, which corresponds to the pH at laboratory temperature (23°C). We observe a good match between the model prediction (solid line in Figure 3a) and our measured data, which we recognize is nonunique as there are multiple parameters that can be adjusted in the model over the range reasonable for silica in contact with NaCl electrolyte. The key point is that a reasonable match can only be obtained if the temperature dependence of pH is accounted for. Assuming constant pH yields a zeta potential that increases in magnitude with increasing temperature (dashed line in Figure 3a).

There are no published experimental data against which we can compare the results obtained here at 0.5 M, and the model of *Revil et al*. [1999] is not valid at such high ionic strength. However, *Saunders et al*. [2012] predicted that the zeta potential of sandstone saturated with NaCl electrolyte is insensitive to temperature at ionic strength greater than about 0.3 M based on the following argument. Above approximately 0.3 M, it has been shown that the magnitude of the zeta potential at laboratory temperature in sandstones saturated with NaCl electrolyte no longer decreases with increasing ionic strength [*Jaafar et al*., 2009]. Moreover, it has been suggested that the maximum packing of Na^+ counterions within the diffuse layer is reached at this ionic strength [*Vinogradov et al*., 2010]. As the ionic strength increases beyond this point, the counterion density within the double layer remains constant, so the zeta potential also remains constant [see, for example, *Vinogradov et al*., 2010, Figure 11a]. *Saunders et al*. [2012] argued that the physical size of ions is expected to be only weakly temperature dependent, so the same limiting minimum value of zeta potential may be used at all temperatures if the ionic strength is greater than about 0.3 M. *Jaafar et al*. [2009] found that the limiting minimum zeta potential at laboratory temperature was approximately −17 mV, while *Vinogradov et al*. [2010] found that it was -13.5 ± 3.5 mV. Data from *Walker et al*. [2014] also suggest a minimum limiting zeta potential of -13 ± 3 mV. Here we find a limiting minimum zeta potential of -9.5 ± 1 mV that is independent of temperature, consistent with those obtained previously at laboratory temperature within experimental error, and with the prediction of the simple model of *Saunders et al*. [2012]. However, it should be noted that this model neglects the effect of varying pH.

In the data reported here we observe a strong correlation between zeta potential and pH. At the lower ionic strength investigated, pH and zeta potential both decrease with increasing temperature; conversely, at the higher ionic strength, the pH and zeta potential are both constant and independent of temperature. Figure 3c shows the zeta potential plotted against pH. A linear regression matches most of the data at lower ionic strength within experimental error and yields a good quality of fit with $R^2 = 0.92$. The data at higher ionic strength clusters around the mean pH and zeta potential values of 7.3 and −9.5 mV, respectively, and these mean values match most of the data within experimental error. It is well known that pH controls the surface charge of metal oxides such as quartz, and we hypothesize that the temperature dependence of the zeta potential observed here is primarily caused by the temperature dependence of the electrolyte pH. This hypothesis is supported by the experimental data we report here, and also by much of the previously published data. It can also explain the apparently contradictory behavior observed previously.

In unbuffered experiments in which the pH is not externally controlled, the pH and zeta potential at low ionic strength both decrease in magnitude with increasing temperature. Such behavior is demonstrated here and was also observed by *Dunstan* [1994], although they did not test the correlation between pH and zeta potential. It is also consistent with the model of *Revil et al*. [1999] if the temperature dependence of pH is accounted for. In buffered experiments in which the pH is externally controlled, the zeta potential at low ionic strength increases in magnitude with increasing temperature, as observed by *Ishido and Mizutani* [1981] and *Alekhin et al*. [1984] and consistent with the model of *Revil et al*. [1999] if the fixed pH is accounted for. In both buffered and unbuffered experiments at high ionic strength, the pH and zeta potential remain constant and independent of temperature. The constant value of zeta potential depends upon the mineral type, electrolyte composition, and pH and is found here to be -9.5 ± 1 mV in sandstones saturated with NaCl electrolyte at pH 7.3.

The simple model described above, which relates the temperature dependence of the zeta potential to the temperature dependence of pH, explains the experimental results reported here and also the previously published data shown in Figure 1 with the exception of *Reppert and Morgan* [2003] (data sets 1 and 2 in Figure 1 and Table S1). They reported an increase in the magnitude of the zeta potential with increasing temperature, along with a decrease in pH. However, when we calculate the zeta potential corresponding to data sets 1 and 2 using equation (1) and values of the streaming potential coupling coefficient, saturated rock conductivity and formation factor reported by *Reppert and Morgan* [2003], we find that the temperature dependence of the zeta potential is consistent with our observations and the simple model outlined above (shown as recalculated data sets 1 and 3 in Figure 3a). We cannot explain the discrepancy between the zeta potential reported by *Reppert and Morgan* [2003] and the values we calculate here from their reported experimental data.

The relationship between temperature and electrolyte pH, and hence zeta potential, is still poorly understood. *Millero et al*. [2009] reported similar behavior to that observed here, but the measurements were conducted on NaCl electrolyte alone with no minerals present, and the decrease in pH was attributed solely to enhanced dissociation of water molecules with increasing temperature. Moreover, *Glover et al*. [2012] predicted a similar decrease in pH with increasing temperature owing to enhanced dissociation of water molecules and pointed out that electrolyte pH is also expected to decrease with increasing temperature as a result of increased dissolution of atmospheric CO_2 in the electrolyte. However, we carried out closed system experiments with minimal exposure of the electrolyte to atmosphere, consistent with deep subsurface settings. We hypothesize that in addition to the dissociation of water molecules, some ion exchange occurs with the mineral surfaces in our sandstone samples, with a proton from the silanol group being replaced by a Na^+ ion from the solution (as suggested by *Revil et al*. [1999]). This further reduces the brine pH and results in a more positive zeta potential (i.e., the negative zeta potential reduces in magnitude) as observed in numerous previous studies [e.g., *Kosmulski and Matijević*, 1992]. This hypothesis is supported by the observation that some of the change in electrolyte pH in our experiments was irreversible: the pH did not return to its original value at laboratory conditions. For example, the pH of the 0.01 M NaCl electrolyte remained 1 pH unit lower than the initial value after conducting experiments at 80°C. Moreover, the same electrolyte showed no such irreversible change when heated to 80°C without contact with the sandstone samples. Changes in electrolyte pH resulting only from enhanced dissociation of water molecules or CO_2 dissolution at elevated temperature would be

similar irrespective of whether the sample was in contact with the sandstone samples, which was not the case here. The irreversible pH change observed when the electrolyte is in contact with the samples supports our hypothesis of ion exchange on the mineral surfaces.

The relationships between zeta potential, temperature, and electrolyte ionic strength and pH reported in this study are important for many subsurface applications. For example, many deep sandstone reservoirs relevant to hydrocarbon production or CO_2 storage, or sandstones in hydrothermal fields, are at temperatures >80°C. At low ionic strength, and in the absence of any pH buffers such as calcite or clay minerals, the zeta potential may be considerably lower than that measured in experiments at laboratory conditions. Conversely, if the pH is buffered and the value was known and correctly reproduced in laboratory conditions, the zeta potential in situ may be considerably higher than that measured at laboratory conditions. Measurements of the in situ pH in such systems are essential in order to predict correctly the zeta potential. At high ionic strength, the zeta potential is insensitive to temperature and, for a given value of pH, measurements at laboratory conditions may be applied in situ.

5. Conclusions

We find that the temperature dependence of the (negative) zeta potential in natural sandstones saturated with NaCl electrolyte depends on ionic strength. At low ionic strength (<0.5 M), the zeta potential decreases in magnitude with increasing temperature; at high ionic strength (>0.5 M), the zeta potential is independent of temperature. Moreover, at low ionic strength, the pH also decreases with increasing temperature, but at high ionic strength the pH remains constant. The temperature dependence of the zeta potential can be explained by the temperature dependence of the pH, which is well known to control the surface charge of metal oxides such as quartz. Our findings are consistent with published models of the zeta potential, so long as the temperature dependence of the pH at low ionic strength is accounted for. Moreover, they explain the hitherto contradictory results reported in previous studies that used low ionic strength electrolytes. In unbuffered experiments, the pH decreases with increasing temperature, and the zeta potential decreases in magnitude, while in experiments with fixed pH, the zeta potential increases in magnitude with increasing temperature. The results have broad application to deep sandstone reservoirs and hydrothermal fields.

Acknowledgments

Supporting data are included in PDF and CSV files; any additional data may be obtained from the corresponding author (e-mail: j.vinogradov@imperial.ac.uk). TOTAL is thanked for partial support of Jackson's Chair in Geological Fluid Mechanics and for supporting the activities of the TOTAL Laboratory for Reservoir Physics at Imperial College London where these experiments were conducted.

The Editor thanks Andre Revil and Paul Glover for their assistance in evaluating this paper.

References

Alekhin, Y. V., M. P. Sidorova, L. I. Ivanova, and L. Z. Lakshtanov (1984), Investigation of the electrokinetic potential and adsorption of ions on Al_2O_3 and SiO_2 at high temperature and pressures, *Kolloidn. Zh.*, *46*, 1195–1198.

Aubert, M., and Q. Y. Atangana (1996), Self-potential method in hydrogeological exploration of volcanic areas, *Groundwater*, *34*, 1010–1016, doi:10.1111/j.1745-6584.1996.tb02166.x.

Corwin, R. F., and D. B. Hoover (1979), The self-potential method in geothermal exploration, *Geophysics*, *44*, 226–245, doi:10.1190/1.1440964.

Darnet, M., Maineult, A., G. Marquis (2004), On the origins of self-potential (SP) anomalies induced by water injections into geothermal reservoirs, *Geophys. Res. Lett.*, *31*, L19609, doi:10.1029/2004GL020922.

Dunstan, D. E. (1994), Temperature-dependence of the electrokinetic properties of two disparate surfaces, *J. Colloid Interface Sci.*, *166*, 472–475, doi:10.1006/jcis.1994.1319.

Fairbrother, F., and H. Mastin (1924), Studies in electro-endosmosis, *J. Chem. Soc. Trans.*, *125*, 2319–2330, doi:10.1039/CT9242502319.

Fitterman, D. V., and R. F. Corwin (1982), Inversion of self-potential data from the Cerro Prieto geothermal field, Mexico, *Geophysics*, *47*, 938–945, doi:10.1190/1.1441361.

Glover, P. W. J. (2015), Geophysical properties of the near surface Earth: Electrical properties, in *Treatise on Geophysics*, vol. 11, 2nd ed., edited by G. Schubert, pp. 89–137, Elsevier, Oxford.

Glover, P. W. J., and N. Déry (2010), Dependence of streaming potential on grain diameter and pore radius for quartz glass beads, *Geophysics*, *75*(6), F225–F241, doi:10.1190/1.3509465.

Glover, P. W. J., E. Walker, and M. D. Jackson (2012), Streaming-potential coefficient of reservoir rock: A theoretical model, *Geophysics*, *77*(2), D17–D43, doi:10.1190/geo2011-0364.1.

Gulamali, M. Z., E. Leinov, and M. D. Jackson (2011), Self-potential anomalies induced by water injection into hydrocarbon reservoirs, *Geophysics*, *76*, F283–F292, doi:10.1190/1.3596010.

Ishido, T., and H. Mizutani (1981), Experimental and theoretical basis of electrokinetic phenomena in rock-water systems and its applications to geophysics, *J. Geophys. Res.*, *86*(B3), 1763–1775, doi:10.1029/JB086iB03p01763.

Ishido, T., T. Kikuchi, and M. Sugihara, (1989), Mapping thermally driven upflows by the self-potential method, in *Hydrogeological Regimes and Their Subsurface Thermal Effects*, edited by A. E. Beck, G. Garven, and L. Stegena, AGU, Washington, D. C., doi:10.1029/GM047p0151.

Ishido, T., J. W. Pritchett, T. Tosha, Y. Nishi, and S. Nakanishi (2013), Monitoring underground migration of sequestered CO_2 using self-potential methods, *Energy Procedia*, *37*, 4077–4084, doi:10.1016/j.egypro.2013.06.308.

Jaafar, M. Z., J. Vinogradov, and M. D. Jackson (2009), Measurement of streaming potential coupling coefficient in sandstones saturated with high salinity NaCl brine, *Geophys. Res. Lett.*, *36*, L21306, doi:10.1029/2009GL040549.

Jackson, M. D. (2015), Self-potential: Tools and techniques, in *Treatise on Geophysics*, vol. 11, 2nd ed., edited by G. Schubert, chap. 9, Elsevier, Oxford.

Jackson, M. D., and J. Vinogradov (2012), Impact of wettability on laboratory measurements of streaming potential in carbonates, *Colloid. Surface. Physicochem. Eng. Aspect.*, *393*, doi:10.1016/j.colsurfa.2011.11.00.

Jardani, A., A. Revil A. Bolève, and J. P. Dupont (2008), Three-dimensional inversion of self-potential data used to constrain the pattern of groundwater flow in geothermal fields, *J. Geophys. Res.*, *113*, B09204, doi:10.1029/2007JB005302.

Jouniaux, L., and J. P. Pozzi (1995), Streaming potential and permeability of saturated sandstones under triaxial stress: Consequences for electrotelluric anomalies prior to earthquakes, *J. Geophys. Res.*, *100*(B6), 10,197–10,209, doi:10.1029/95JB00069.

Kosmulski, M., and E. Matijević (1992), Formation of the surface charge on silica in mixed solvents, *Colloid Polym. Sci.*, *270*(10), 1046–1048, doi:10.1007/BF00655975.

Leinov, E., and M. D. Jackson (2014), Experimental measurements of the SP response to concentration and temperature gradients in sandstones with application to subsurface geophysical monitoring, *J. Geophys. Res. Solid Earth*, *119*, 6855–6876, doi:10.1002/2014JB011249.

Michel, S., and J. Zlotnicki (1998), Self-potential and magnetic surveying of La Fournaise volcano (Réunion Island): Correlations with faulting, fluid circulation, and eruption, *J. Geophys. Res.*, *103*(B8), 17,845–17,857, doi:10.1029/98JB00607.

Millero, F. J., B. DiTrolio, A. F. Suarez, and G. Lando (2009), Spectroscopic measurements of the pH in NaCl brines, *Geochim. Cosmochim. Acta*, *73*(11), 3109–3114, doi:10.1016/j.gca.2009.01.037.

Moore, J. R., S. D. Glaser, H. F. Morrison, and G. M. Hoversten (2004), The streaming potential of liquid carbon dioxide in Berea sandstone, *Geophys. Res. Lett.*, *31*, L17610, doi:10.1029/2004GL020774.

Reppert, P. M., and F. D. Morgan (2003), Temperature-dependent streaming potentials: 2. Laboratory, *J. Geophys. Res.*, *108*(B11), 2547, doi:10.1029/2002JB001755.

Revil, A., and H. Mahardika (2013), Coupled hydromechanical and electromagnetic disturbances in unsaturated porous materials, *Water Resour. Res.*, *49*, doi:10.1002/wrcr.20092.

Revil, A., and P. A. Pezard (1998), Streaming electrical potential anomaly along faults in geothermal areas, *Geophys. Res. Lett.*, *25*(16), 1944–8007, doi:10.1029/98GL02384.

Revil, A., P. A. Pezard, and P. W. J. Glover (1999), Streaming potential in porous media: 1. Theory of the zeta potential, *J. Geophys. Res.*, *104*(B9), 20,021–20,031, doi:10.1029/1999JB900089.

Revil, A., et al. (2011), Hydrogeology of Stromboli volcano, Aeolian Islands (Italy) from the interpretation of resistivity tomograms, self-potential, soil temperature and soil CO_2 concentration measurements, *Geophys. J. Int.*, *186*, 1078–1094, doi:10.1111/j.1365-246X.2011.05112.x.

Saunders, J. H., M. D. Jackson, M. Y. Gulamali, J. Vinogradov, and C. C. Pain (2012), Streaming potentials at hydrocarbon reservoir conditions, *Geophysics*, *77*, E77–E90, doi:10.1190/geo2011-0068.1.

Vinogradov, J., and M. D. Jackson (2011), Multiphase streaming potential in sandstones saturated with gas/brine and oil/brine during drainage and imbibition, *Geophys. Res. Lett.*, *38*, L01301, doi:10.1029/2010GL045726.

Vinogradov, J., M. Z. Jaafar, and M. D. Jackson (2010), Measurement of streaming potential coupling coefficient in sandstones saturated with natural and artificial brines at high salinity, *J. Geophys. Res.*, *115*, B12204, doi:10.1029/2010JB007593.

Walker, E., P. W. J. Glover, and J. Ruel (2014), A transient method for measuring the DC streaming potential coefficient of porous and fractured rocks, *J. Geophys. Res. Solid Earth*, *119*, 957–970, doi:10.1002/2013JB010579.